

RSC Advances



This article can be cited before page numbers have been issued, to do this please use: M. malmir, A. Elhampour, E. kowsari, F. borbor and F. Nemat, *RSC Adv.*, 2016, DOI: 10.1039/C6RA18810A.



This is an *Accepted Manuscript*, which has been through the Royal Society of Chemistry peer review process and has been accepted for publication.

Accepted Manuscripts are published online shortly after acceptance, before technical editing, formatting and proof reading. Using this free service, authors can make their results available to the community, in citable form, before we publish the edited article. This *Accepted Manuscript* will be replaced by the edited, formatted and paginated article as soon as this is available.

You can find more information about *Accepted Manuscripts* in the [Information for Authors](#).

Please note that technical editing may introduce minor changes to the text and/or graphics, which may alter content. The journal's standard [Terms & Conditions](#) and the [Ethical guidelines](#) still apply. In no event shall the Royal Society of Chemistry be held responsible for any errors or omissions in this *Accepted Manuscript* or any consequences arising from the use of any information it contains.

Ag-doped Nano Magnetic γ -Fe₂O₃@DA Core–Shell Hollow Spheres: an efficient and recoverable heterogeneous catalyst for A³, KA² Coupling Reactions and [3+2] cycloaddition

Received 00th January 20xx,
Accepted 00th January 20xx

DOI: 10.1039/x0xx00000x

www.rsc.org/

A. Elhampour,^{a,*} M. Malmir,^{b,*} E. Kowsari,^b F. Boorboor ajdari^b and F. Nemati^a

An effective protocol for the fabrication of Ag-doped Nano Magnetic γ -Fe₂O₃@DA Core-Shell Hollow Spheres (h-Fe₂O₃@DA/Ag), by a simple hydrothermal method demonstrated without any templates in the reaction system. The synthesized core-shell structure was successfully characterized in terms of the chemical composition, surface morphology, and magnet properties by using: FT-IR, VSM, TGA, TEM, FE-SEM, EDS, and XRD patterns. The possible formation mechanism of this magnetic γ -Fe₂O₃@DA/Ag hollow sphere structure described based on the experimental results. In addition, as physical property, apparent shell density was determined using specific surface area (BET) and shell thickness (BJH). An important, the novel and unique catalyst with hollow structural characters and strong magnetic behavior, exhibited high performance catalytic activity in the A³, KA² coupling reactions and [3+2] cycloaddition for the synthesis of 1H-tetrazoles. Furthermore, facilitated recovering by the well manner from the reaction mixture by magnetic field and multiple recycling without any significant loss in catalytic activity.

Introduction

Regarding to future technologies and exploring facile, safe and economic methods for the synthesis of magnetic materials has spurred intense and rapid development in the field of material science.^{1,2} Particularly, iron oxide-based magnetic materials have been extensively pursued for multidisciplinary researches, due to their physical and chemical properties and technical applications.^{3,4} As one of the most important, inexpensive, non-toxic, nature-friendly, and the most stable phase of iron oxides, maghemite (γ -Fe₂O₃), has become an attractive material. And also, many techniques including vapor-solid growth,⁵⁻⁷ template aimed synthesis,⁸ sol-gel process,⁹ and hydrothermal synthesis¹⁰⁻¹² have been directed to prepare various types of Fe₂O₃ crystals. To date, much attentions have been focused on the size and functionalization of iron oxide nanoparticles with various morphologies such as nanorods, nanowires, nanocubics and etc.^{10,13-16} lately, hollow structures with high surface area, low material density as well as strong magnetic response and good permeation have attracted many attentions as an important solution in controlled drug delivery, sensors, lightweight fillers, catalysis.¹⁷⁻¹⁹ Notably, they could be manipulated by an external magnetic field.²⁰ Very recently, several strategies for hollow structures synthesis such as the Ostwald ripening,^{21,22}

Kirkendall effect,²³ molten salt corrosion,²⁴ reverse micelle transport,²⁵ and layer-by-layer assembly²⁶ have been developed. These fabrication approaches are conventionally based on the well-established template methods include: hard-template, soft-template, and sacrificial template.²⁷⁻²⁹ Therefore, developing a facile method becomes the main purpose for the synthesis of magnetic hollow structures. In a sense, preparing nonspherical hollow structures with one-pot template-free method is still a perfect method. During the last decade, different kinds of hollow spheres supported on various materials including organic,^{30,31} inorganic^{32,33} and their hybrid materials³⁴⁻³⁷ was reported. Recently, Hollow magnetic nanoparticles have been also reported as an excellent type of catalyst support because of their good stability, facile synthesis and functionalization process, high specific surface area, low density and facile separation process.^{38,39}

Dopamine (DA) is one of the most significant catecholamine, plays an important role in the functionalizing of the central nervous, cardiovascular, renal, and hormonal systems, as well as in drug addiction and Parkinson's disease.^{40,41} Nowadays, Dopamine derivatives provide a novel and useful alternative for surface immobilization schemes. Obviously, dopamine and its derivatives open a new route to the modification of iron oxide nanoparticles as a novel organic coating material.⁴²⁻⁴⁶ Enhancing of the catalytic activity of DA will be another important property for applications of heterogeneous catalysts in the future. Hence, noble metals such as Ag, Au, Pt, and Pd deposited on dopamine surfaces, enhanced the catalytic activity of dopamine. Also, silver catalyst showed good catalytic activity towards coupling, cycloaddition, sigmatropic rearrangement, cycloisomerization, and nitrene transfer

^a Department of Chemistry, Semnan University, Semnan, Iran, Zip Code: 35131-19111, E-mail: elhampour_ali@yahoo.com

^b Department of Chemistry, Amirkabir University of Technology, Hafez Avenue, No. 424, Tehran, Iran. E-mail: masi.malmir@yahoo.com

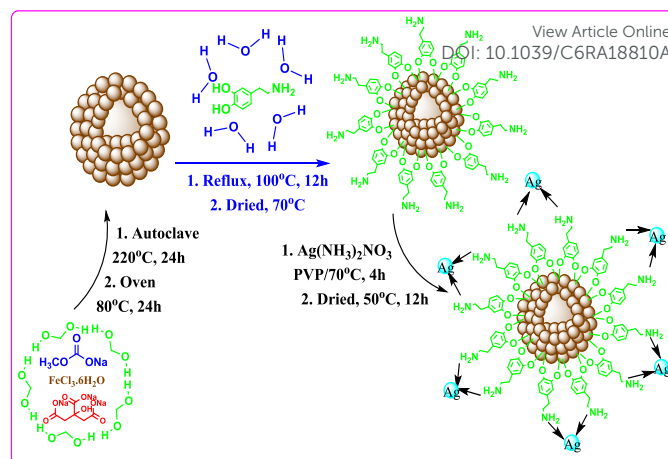
reactions; it has been widely employed.⁴⁷ Among them, A³ coupling reaction (aldehyde, alkyne and amine) has been widely used for the easy formation of high-value product propargylamines *via* C–H bond activation, recently.⁴⁸ Propargylamines are frequently used as synthetically adaptable key intermediates^{49,50} in a synthesis of varied natural products and biologically active compounds and forming of many nitrogen-containing biologically active.⁵¹ Up until now, many methods were carried out by using a wide range of transition metal catalyst such as copper,^{52–54} iridium,⁵⁵ nickel,⁵⁶ and iron⁵⁷ which has been well explored for the synthesis of propargylamines. In addition to the propargylamine, tetrazole is one of the most important intermediate and greater synthetic favorites prepared by [3+2] cycloaddition reaction starting from nitrile. Various synthetic approaches have been disclosed for this transformation.^{58–65} Generally, these catalytic systems suffered from some drawbacks such as: inability of the catalyst for recovering process. So, the development of environmentally friendly synthetic methods involved facile separation of catalysts from the reaction mixture has become increasingly an important argument. Nowadays, the development of environmentally friendly catalyzed MCRs enjoying the easy recovery and effective recyclability of catalysts as well as improving the atom economy is overgrowing, overshadowing and compensating the use of catalysts.^{66–75} Herein, we describe a novel and unique Ag nanoparticles supported on the magnetic Fe₂O₃ core and DA shell hollow sphere structure is an effective and selective catalyst in the A³ coupling, and KA² reaction and [3+2] cycloaddition under mild reaction conditions. The magnetic-Fe₂O₃@DA/Ag hollow sphere was conveniently prepared and its structure was fully characterized by XRD, FT-IR, FE-SEM, TEM, EDS, TGA, and VSM analysis.

Results and discussion

Synthesis of magnetic Fe₂O₃@DA/Ag hollow sphere

The process for the preparation of the magnetic Fe₂O₃@DA/Ag hollow sphere catalyst is schematically described in Scheme 1. The nano magnetic Fe₂O₃@DA/Ag hollow sphere was prepared from commercially inexpensive available materials and fully characterized using, the corresponding data, provided by FT-IR, FE-SEM, TEM, XRD, TGA, and VSM techniques.

As shown in scheme 1, in the first step, Fe₂O₃ hollow sphere were synthesized by hydrothermal treatment.⁷⁶ In the second step, Fe₂O₃ hollow sphere were functionalized with dopamine groups (DA), which the functionalized nanoparticles coated with dopamine (Fe-Ox dopamine) was performed by methods⁶³ but without preliminary functionalization of the terminal amine. Thirdly, Ag(NH₃)₂NO₃ was supported on the surface of a magnetic Fe₂O₃@DA hollow sphere through an *in situ* wet chemistry,⁶⁴ and the silver complex was reduced to Ag(0) particles.



Scheme 1. The possible formation process of Fe₂O₃@DA/Ag hollow spheres

Structure characterization of the magnetic Fe₂O₃@DA/Ag hollow sphere

FT-IR spectra

To clarify the compositions of the synthesized materials, FT-IR was used to characterize the hollow Fe₂O₃, hollow Fe₂O₃@DA and hollow Fe₂O₃@DA doped with Ag nanoparticles in the range of 4000–500 cm⁻¹ are presented in Fig. 1. In all these spectra, the strong absorption peaks at 480–580 cm⁻¹ are observed. These bands attributed to the Intrinsic stretching vibrations of Fe–O in the hematite particle. The significant features for h-Fe₂O₃@DA spectrum (Fig. 1b) are the appearance of the peaks at 3367, 3095, 1629, 1408 and 1276 cm⁻¹ could be assigned to the –NH₂ and C–N is stretching vibration of dopamine on the surface of magnetic hollow sphere.⁷⁷ From the FT-IR spectra, it can be observed that the magnetic Fe₂O₃ hollow sphere was functionalized by dopamine.

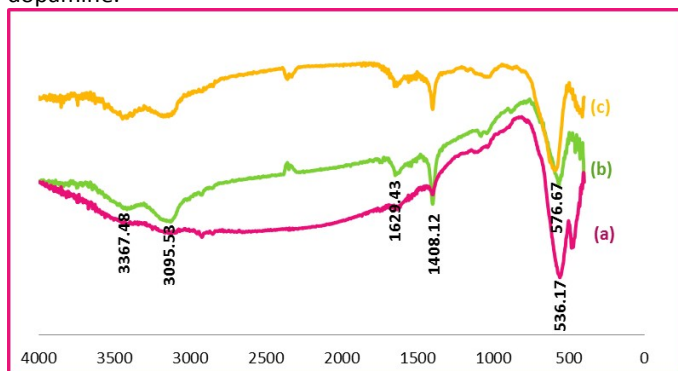


Figure 1. The FT-IR spectra of (a) h-Fe₂O₃, (b) h-Fe₂O₃@DA and (c) h-Fe₂O₃@DA/Ag.

X-ray diffraction spectra

The phase and composition of the as-obtained products were examined by X-ray diffraction (XRD) patterns. Fig. 2 (**Curve 2a**), shows the XRD pattern of magnetic Fe₂O₃ hollow spheres, that the strong diffraction peaks at 30.21, 35.62, 43.34, 53.6, 57.2, 62.83 and 74.5 can be indexed to the {220}, {311}, {400}, {422},

{511}, {440} and {533} planes of typical cubic structure hematite (JCPDS card No. 39-1346) without additional peaks are detected, suggesting high purity of the as-synthesized hematite (labeled as **F**). After coating Fe_2O_3 by dopamine, the broad band appearing in the range from 20° to 25° which is due to the presence of amorphous dopamine shells formed around the magnetic hollow sphere (labeled as **D**). Additionally, based on the diffraction peaks that correspond to h- Fe_2O_3 and DA shell, there are four diffraction peaks else, labeled as **S** in the figure 2c. These diffraction peaks were indexed to the cubic phase of Ag (JCPDS card No. 04-0783) with a lattice constant $a = 2.41 \text{ \AA}$. The mean size of the ordered $\gamma\text{-Fe}_2\text{O}_3$ nanoparticles has been estimated from full width at half maximum (FWHM) and Debye-Sherrer formula according to equation the following:

$$D = \frac{0.89 \lambda}{B \cos \theta}$$

The mean size of as-prepared $\gamma\text{-Fe}_2\text{O}_3$ nanoparticles was around 47 nm from this Debye-Sherrer equation. According to XRD pattern and this investigation, it is clear that maghemite Fe_2O_3 @DA/Ag hollow spheres have been prepared successfully.

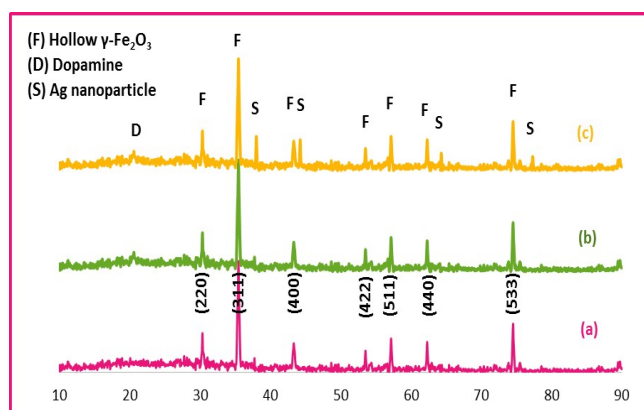


Figure 2. XRD pattern of (a) h- Fe_2O_3 , (b) h- Fe_2O_3 @DA and (c) h- Fe_2O_3 @DA/Ag

TG analyzer

The temperature-dependent changes can be verified by the determination of mass loss employing thermo gravimetric analysis (TGA). The TGA of the synthesis h- Fe_2O_3 and h- Fe_2O_3 @DA/Ag are shown in Fig. 3. As shown in Fig 3a, smaller weight losses below around 200°C are perhaps due to the removal of surface hydroxyls and/or surface adsorbed water, as well as the endothermic weight loss at ($300\text{--}600^\circ\text{C}$) is attributed to water loss from organic groups on the surface. Based on the results displayed in fig 3b, by increasing the temperature a vigorous weight loss for H- Fe_2O_3 @DA/Ag was observed, owing to decomposition of adsorbed organic groups on their surfaces. The removal of organic components starts at around 200°C and is virtually completed at 500°C . Thus, the successful doping of dopamine with Ag nanoparticles on the surface of the hollow- Fe_2O_3 is verified and exhibits a considerable thermal stability at high temperatures.

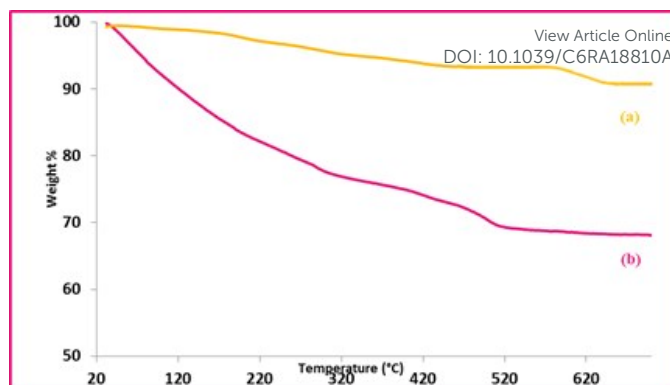


Figure 3. TGA analysis of (a) h- Fe_2O_3 and (b) h- Fe_2O_3 @DA/Ag

Magnetization study

The magnetic properties of the h- Fe_2O_3 , h- Fe_2O_3 @DA and h- Fe_2O_3 @DA/Ag were measured by vibrating sample magnetometer (VSM) at room temperature, as shown in Fig. 4. The maximum saturation magnetization (M_s) values of h- Fe_2O_3 @DA and h- Fe_2O_3 @DA/Ag were found to be 32.35 and 22.63 emu/g, respectively. It is clear that, the M_s value of the corresponding magnetic Fe_2O_3 hollow sphere (45.28 emu/g) is significantly higher than of the h- Fe_2O_3 @DA and h- Fe_2O_3 @DA/Ag sphere, which may be due to the h- Fe_2O_3 were coated with a layer of dopamine in the Fe_2O_3 @DA and Ag-doped nano magnetic Fe_2O_3 @DA/Ag hollow spheres. In addition, it can be seen that there are no obvious changes in the coercivity from the enlarged view of the central loop of the samples. The result demonstrates that the as synthesized Fe_2O_3 @DA/Ag hollow spheres presents excellent magnetic separation properties and have high potential in applications as recyclable nano catalysts and facile separation from the solution with the help of an external magnetic force.

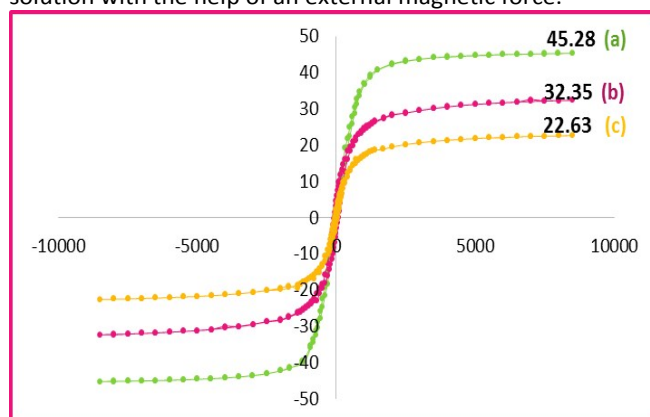


Figure 4. The magnetization curves of (a) h- Fe_2O_3 , (b) h- Fe_2O_3 @DA and (c) h- Fe_2O_3 @DA/Ag

FE-SEM-EDS and TEM analysis

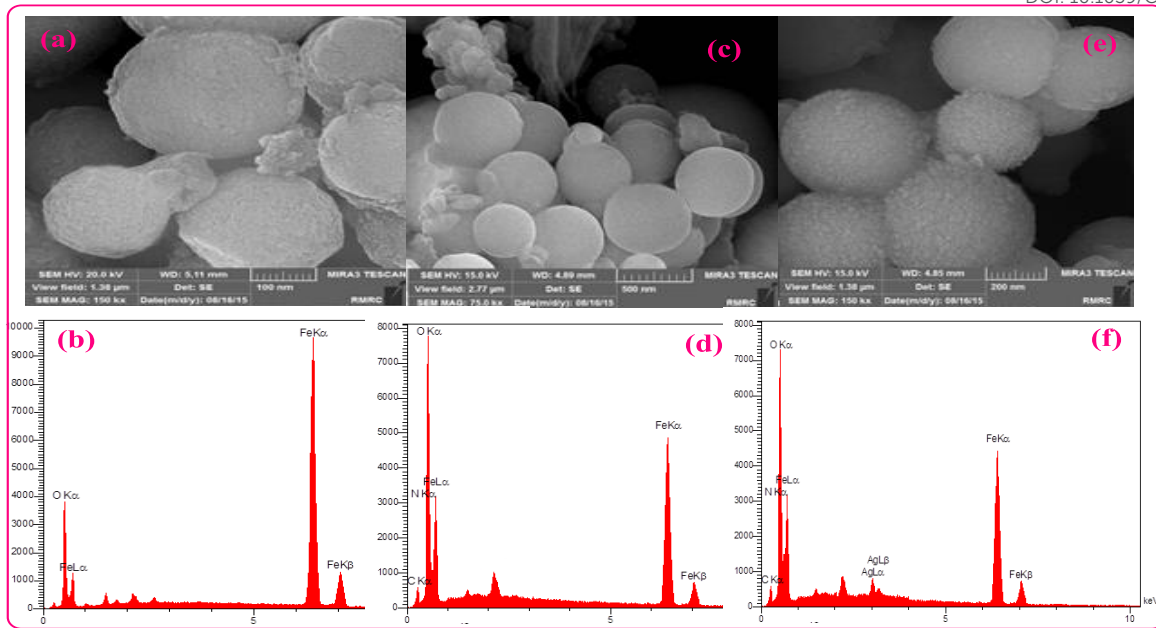
View Article Online
DOI: 10.1039/C6RA18810A

Figure 5. The FEG-SEM-EDS analysis of (a,b) $h\text{-Fe}_2\text{O}_3$, (c,d) $h\text{-Fe}_2\text{O}_3@DA$ and (e,f) $h\text{-Fe}_2\text{O}_3@DA/Ag$

The morphology and structure of the obtained $h\text{-Fe}_2\text{O}_3$, $h\text{-Fe}_2\text{O}_3@DA$ and $h\text{-Fe}_2\text{O}_3@DA/Ag$ were investigated by FE-SEM, EDS and TEM analysis to characterize the resultant products at different stages during the course of synthesis (Fig. 5). From Fig. 5a, b and c, it can be clearly observed that the nano magnetic Fe_2O_3 are spherical in shape with an average diameter of 400 nm. From the FE-SEM image shown in Figure 5a with the significant magnification (Fig. 4a), the surface morphology was clearly revealed. After that, the surface of Fe_2O_3 hollow spheres was subsequently modified with a layer of dopamine group. Clearly, the DA layer was formed *via* tiny shelled on the surface of Fe_2O_3 hollow sphere and it is noteworthy; that the presence of the DA shell was efficient in working as a capping agent to stabilize the nanoparticles. On the other hand, the EDS pattern of $\text{Fe}_2\text{O}_3@DA$ hollow spheres confirms the existence of a DA layer (Fig. 5c and d). Finally, in order to prepare $h\text{-Fe}_2\text{O}_3@DA/Ag$ core shell structure, Ag ions adsorbed on $\text{Fe}_2\text{O}_3@DA$ hollow sphere through an in situ wet chemistry. Based on the Figure 5c, the surfaces of the DA shell

are covered with medial quantities of small particles. As expected, the corresponding EDS pattern revealed the presence of Fe, O, N, C and Ag in the structure. Furthermore, based on TEM image (6) and EDS, products were covered by Ag nanoparticles. In addition, EDS results indicated that the loading capacity of the Ag nanoparticles on the support is 4.42 wt%.

To confirm further successfully functionalized fertilizer, the final sample was determined by TEM observations. Generally, From the TEM image (Figure 6), the magnetic cores are black spheres, and a thin gray color shell with an average thickness of about 10 nm appears around the core. It should be noted that the Ag nanoparticles could be observed with an average diameter of about 10-20 nm and homogeneously immobilized on the surface of $\text{Fe}_2\text{O}_3@DA$ hollow spheres. Hence, the successful functionalization of $\text{Fe}_2\text{O}_3@DA$ hollow sphere by DA and Ag nanoparticles is obviously evidenced based on the images examined by TEM observation.

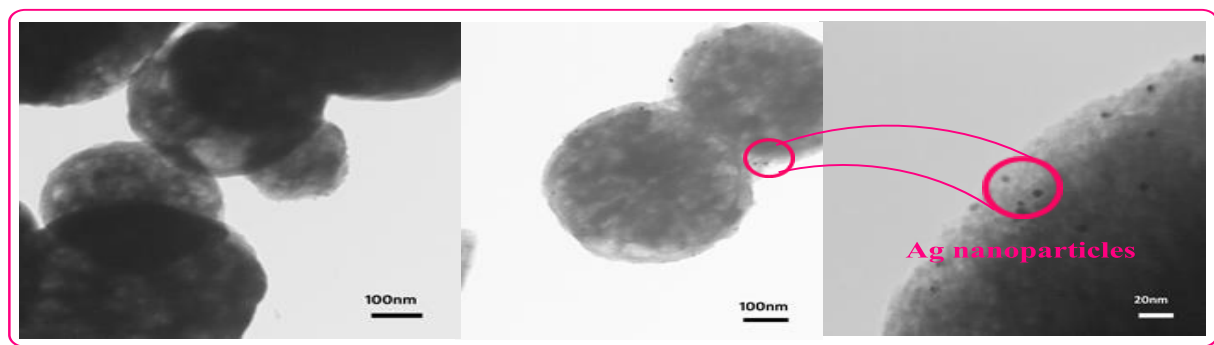


Figure 6. The TEM image of $h\text{-Fe}_2\text{O}_3@DA/Ag$

Determination of the physical property of shell in hollow-sphere

Determination of the physical property of shell in hollow-sphere particles is important since it is a factor which directly affects the functionality of the desired catalyst. Thus we determined the shell density using specific surface area and shell thickness in accordance with the method developed and reported previously.⁷⁸

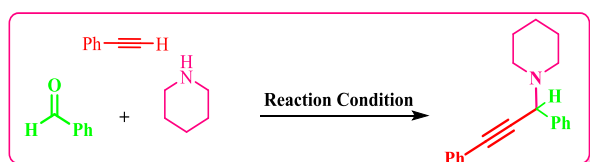
$$S_A = \frac{4\pi\{(r+t)^2+r^2\}}{(4/3)\pi\rho_{\text{shell}}\{(r+t)^3-r^3\}}$$

The ρ_{shell} was calculated with a shell thickness of t (nm) (obtained from XRD), the inner radius of r (nm) (obtained from BET)⁷⁶ and specific surface area S_A ($\text{m}^2\cdot\text{g}^{-1}$) (obtained from BJH).⁷⁶ Therefore the ρ_{shell} value was calculated to be $2.9 \text{ g}\cdot\text{cm}^{-3}$. The magnetite's density is established at $3.25 \text{ g}\cdot\text{cm}^{-3}$, therefore the as-synthesized hollow spheres have lower density than solid sphere-like Fe_2O_3 which show they have a good potential being applied at industrial levels.

Catalytic activity of nano magnetic $\text{Fe}_2\text{O}_3@DA/Ag$ hollow sphere

Catalytic performance of nano magnetic $\text{Fe}_2\text{O}_3@DA/Ag$ hollow sphere in A^3 coupling and KA^2 reaction

Achieving successfully synthesized and characterization of catalyst, its role as a catalyst was evaluated in A^3 and KA^2 coupling reactions. At first, the proper reaction was chosen based on the treatment of benzaldehydes (1.0 mmol), piperidine (1.2 mmol) and phenyl acetylene (1.5 mmol) (scheme 2). Figure 7 summarizes the catalytic performances of the catalyst with various parameters such as solvent temperature and the amount of catalyst in this reaction. Then, the model reaction was carried out in the presence of different loading of catalyst. The catalytic activity first increased with the increase of the $h\text{-Fe}_2\text{O}_3@DA/Ag$ loading up to 10 mg. However, the activity decreased with further increases in catalyst loading up to 15 mg. The optimal catalyst loading was determined to be 10 mg. Besides the $h\text{-Fe}_2\text{O}_3@DA/Ag$ loading, and also the effects of reaction solvents, temperatures on the catalytic efficiency were investigated. The above experiment was also performed in various solvents including water, ethanol and dimethylsulfoxide (DMSO), that the yields were lower. Whereas, the best result with highest yield was achieved by carrying out the reaction under solvent free condition.



Scheme 2. Model reaction

Finally, in order to study the effect of temperature on the synthesis of propargylamine, the synthesis of **5a** at various temperatures was

View Article Online
DOI: 10.1039/C6RA18810A

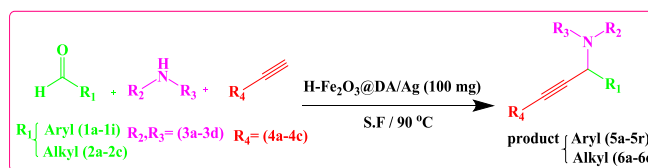


Table 1 Synthesis of three-component reaction of derivatives aldehyde, secondary- amines and terminal alkynes catalyzed by $h\text{-Fe}_2\text{O}_3@DA/Ag$ ^a

R ₁	R ₂	R ₃	R ₄	Product	Time (min)	Yield ^b (%)
1a: C ₆ H ₅	3a: -(CH ₂) ₅ -	4a: C ₆ H ₅		5a	60	98
1b: <i>p</i> -Cl-C ₆ H ₄	3a	4a		5b	60	93
1c: <i>o</i> -Cl-C ₆ H ₄	3a	4a		5c	60	90
1d: <i>p</i> -Br-C ₆ H ₄	3a	4a		5d	60	90
1e: <i>p</i> -Me-C ₆ H ₄	3a	4a		5e	65	91
1f: <i>p</i> -MeO-C ₆ H ₄	3a	4a		5f	65	87
1g: <i>o</i> -Thiophen	3a	4a		5g	60	94
1h: <i>p</i> -OHCC ₆ H ₄	3a	4a		5h	75	90
1i: <i>o</i> -Naphthyl	3a	4a		5i	50	93
1a	3a	4b: <i>p</i> -CH ₃ -C ₆ H ₄		5j	75	88
1a	3a	4c: <i>p</i> -F-C ₆ H ₄		5k	85	80
1a	3b: -(CH ₂) ₂ -O-(CH ₂) ₂ -	4a		5l	60	96
1b	3b	4a		5m	70	90
1e	3b	4a		5n	70	89
1d	3b	4a		5o	65	88
1a	3b	4b		5p	70	90
1a	3c: -(CH ₂) ₄ -	4a		5q	65	80
1a	3d: C ₂ H ₅ C ₂ H ₅	4a		5r	60	70
2a: H	3a	4a		6a	40	90
2a	3a	4b		6b	40	81
2a	3b	4a		6c	40	95
2a	3c	4a		6d	40	85
2a	3d	4a		6e	45	78
2b: C ₆ H ₁₁	3a	4a		6f	45	90
2b	3b	4b		6g	45	85
2b	3b	4a		6h	45	88
2b	3c	4a		6i	45	85
2b	3d	4a		6j	45	65
2b	3a	4c		6k	45	81
2c: -(CH ₂) ₂ -Me	3a	4a		6l	45	90
2c	3b	4a		6m	45	85
2c	3c	4a		6n	45	80
2c	3d	4a		6o	45	75

^a Reaction conditions: aliphatic aldehyde (1.1 mmol) or arylaldehydes (1 mmol), amines (1.1 mmol), alkynes (1.2 mmol), $h\text{-Fe}_2\text{O}_3@DA/Ag$ (10 mg) under solvent-free conditions at 90 °C.

^b Isolated yield.

^c Aqueous formaldehyde (37%, 0.4 mL).

carried out and the results were summarized in figure 7. When the reaction was performed at room temperature, only a trace of the desired product was formed during 5h (green column). On the other hand, at 50 and 90 °C, (yellow and pink column), the product yield decreased. As results, the reaction temperature 90 °C was chosen for subsequent experiments.

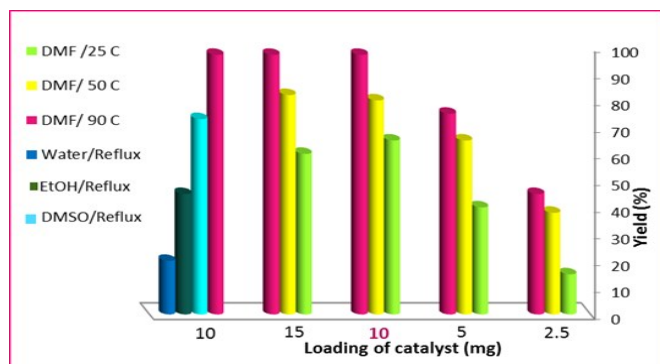


Figure 7. Effects of loading of catalyst, duration of reaction and solvent for the synthesis of propargylamine (Scheme 2)

Thus, the optimized reaction conditions include 1.0 mmol of benzaldehyde, 1.2 mmol of piperidine, 1.5 mmol of phenyl acetylene and 10 mg nano magnetic Fe_2O_3 @DA/Ag hollow sphere of catalyst, at 90 °C under solvent free condition. Encouraged by these results, with the optimized reaction conditions in hand, we initiated our investigation into the scope of aldehydes, amines, and terminal alkynes applicable to the present A^3 coupling reaction and the results are summarized in Table 1. According to these results it was found that, the aromatic aldehydes and aryl acetylenes bearing electron-donating substituents as well as electron-withdrawing groups and aliphatic aldehydes provided the desired products in moderate to high yields within short reaction time.

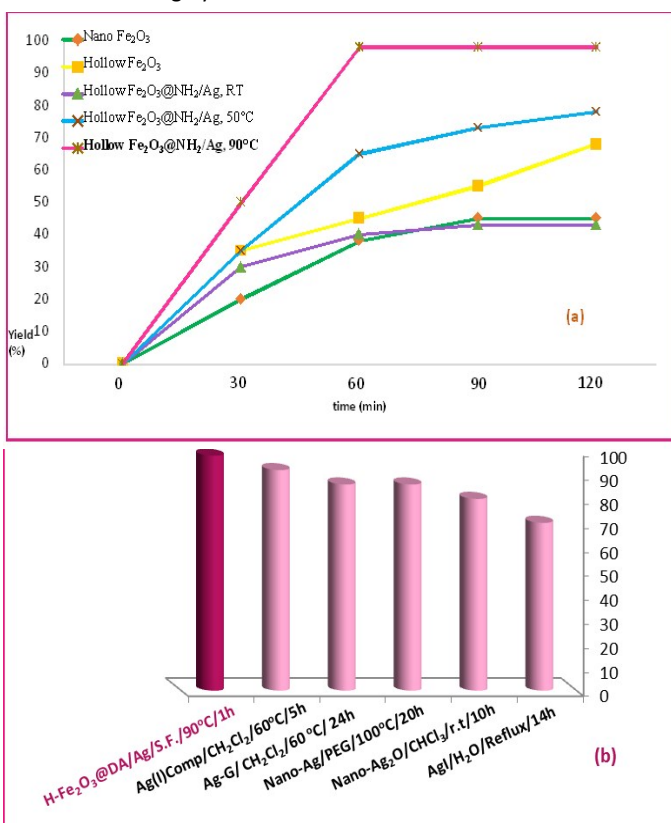
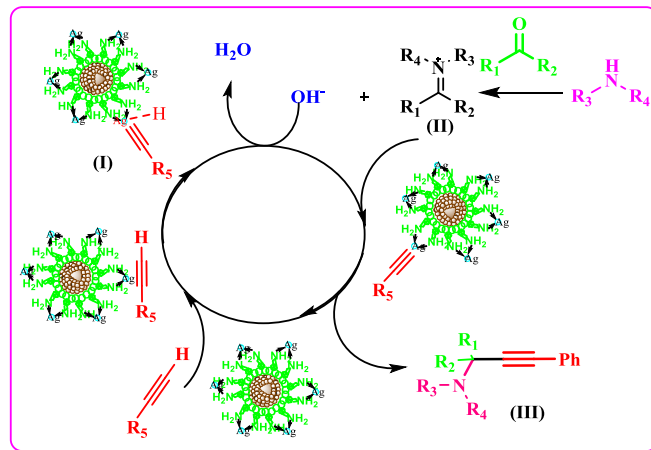


Figure 8. Comparison of $\text{h-Fe}_2\text{O}_3$ @DA/Ag with various $\gamma\text{-Fe}_2\text{O}_3$ catalysts (a) and other recently reported silver catalyst (b) in the preparation of propargylamine (scheme 2)

As demonstrated in Table 1, the cyclic amines such as morpholine and pyrrolidine gave similar results to those obtained with piperidine, whereas diethylamine rendered the corresponding product in modest yield. In order to obtain better results, we carried out a synthesis of **5a** using nano $\gamma\text{-Fe}_2\text{O}_3$ and hollow $\gamma\text{-Fe}_2\text{O}_3$ catalyst to compare the catalytic activity of prepared nano magnetic $\gamma\text{-Fe}_2\text{O}_3$ @DA/Ag hollow sphere as a catalyst under solvent-free conditions from the above observations in figure 8a.

It is clear that nano magnetic Fe_2O_3 @DA/Ag hollow sphere plays a main role compared to other catalysts, due to its nano active surface and high performance of Ag nanoparticles. Also, to show the superiority of the present method over previous ones, we compared our results with some other results reported in the literatures⁷⁹⁻⁸³ (Fig. 8b). Therefore, the $\text{h-Fe}_2\text{O}_3$ @DA/Ag was used as catalyst for the synthesis of propargylamine. As shown, magnetic $\gamma\text{-Fe}_2\text{O}_3$ @DA/Ag hollow sphere as a simple catalyst has several advantages such as short reaction times, excellent yields, simple recovery of magnetic catalyst and avoiding the use of solvent in the reaction system.

A possible mechanism was proposed based on reported literature.⁸¹ According to figure 6, the role of Ag nanoparticles as a Lewis acid catalyst in the synthesis of propargylamine is shown which the immobilized Ag nanoparticles on the surface of $\gamma\text{-Fe}_2\text{O}_3$ @DA hollow sphere insert in terminal alkyne to form the Ag acetylide intermediate (I) with the activation of C-H bond. Meanwhile, the nucleophilic addition of amine to aldehyde leads to generate iminium ion (II). Thus, the silver acetylide intermediate attacks the iminium ion *in situ*, to obtain the corresponding propargylamine (III).



Scheme 3. Plausible mechanism of the A^3 -coupling reaction by $\text{h-Fe}_2\text{O}_3$ @DA/Ag

In order to show the practical applicability of the nano magnetic $\gamma\text{-Fe}_2\text{O}_3$ @DA/Ag hollow sphere, the synthesis of propargylamines of three components coupling reaction of Secondary amines, aliphatic ketones and aryl acetylene (KA^2 reaction) was examined. Importantly, Ketoimines are considered to be less reactive towards nucleophilic additions than aldimines, due to the steric hindrance and electronic effects. Therefore, the utilization of *in situ* generation of ketoimines some reactions, including in the direct alkyne addition reaction still remains a significant challenge for

chemists which should be circumvented.⁸⁴ So, the catalytic activity of the catalyst was tested by the model reaction of cyclohexanone (1.5 mmol), phenyl acetylene (1.5 mmol) and piperidine (1 mmol) to obtain **5a** using 10 mg nano magnetic Fe₂O₃@DA/Ag hollow sphere under similar optimized reaction conditions. The scope of the KA² coupling reaction was evaluated using cyclic ketones, secondary amines and alkynes, applying the optimal condition, and exhibited good reactivity (Table 2). However, the reaction proceeds were utilized cyclic ketones, giving the corresponding propargylamines in high yields. Notably, aromatic ketones gave none of the desired product in long reaction time processes.

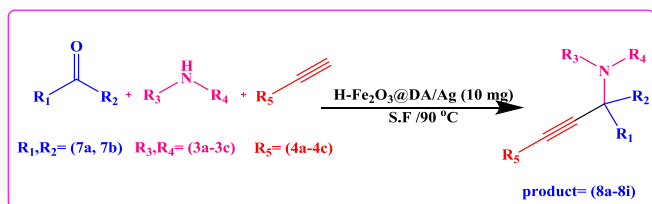


Table 2 Synthesis of the three-component reaction of aliphatic ketones, secondary- amines and terminal alkynes catalysed by h-Fe₂O₃@DA/Ag^a

R ₁ , R ₂	R ₃ , R ₄	R ₅	Prod uct	Time (min)	Yield ^b (%)
7a : -(CH ₂) ₄ -	3a : -(CH ₂) ₅ -	4a : C ₆ H ₅	8a	120	90
7a	3b : -(CH ₂) ₂ -O-(CH ₂) ₂ -	4a	8b	120	85
7a	3c : -(CH ₂) ₄ -	4a	8c	140	82
7b : -(CH ₂) ₅ -	3a	4a	8d	150	87
7b	3a	4b : <i>p</i> -CH ₃ -C ₆ H ₄	8e	175	81
7b	3b	4a	8f	130	92
7b	3b	4b	8g	170	89
7b	3c	4a	8h	140	90
7b	3b	4c : <i>p</i> -F-C ₆ H ₄	8i	145	82

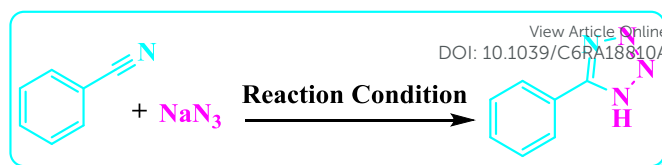
^a Reaction conditions: ketones (1.5 mmol), amines (1 mmol), alkynes (1.5 mmol), h-Fe₂O₃@DA/Ag (10 mg) under solvent-free conditions at 90 °C.

^b Isolated yield

Catalytic testing for synthesis of 1H-Tetrazole in [3+2] cycloaddition

To achieve better results catalytic activity of nano magnetic Fe₂O₃@DA/Ag hollow sphere, its role as a catalyst was evaluated for the synthesis of tetrazoles (scheme 4).

At the beginning, the standard reaction was chosen for the treatment of benzonitrile and sodium azide. Then, this reaction was carried out with various amounts of catalysts, solvents and at different reaction temperature (Fig. 9). To investigate the effect catalyst loading, the model reaction was carried out in the presence of different amount of this.



Scheme 4. Synthesis of 5-Substituted 1H-Tetrazoles by h-Fe₂O₃@DA/Ag

To investigate the effect catalyst loading, the model reaction was carried out in the presence of different amount of catalyst. Hence 30 mg of h-Fe₂O₃@DA/Ag can be catalyzed in [3+2] cycloaddition reactions for synthesis of tetrazoles. More amount of the catalyst has no significant change for the yield of tetrazoles, whereas decreasing the amount of h-Fe₂O₃@DA/Ag lead to decrease the yield a lot. Experiments with different aprotic and protic solvents and solvent free condition revealed the best results in DMF as solvent (blue column) as indicated in figure 9. Water was not a suitable solvent for this reaction, but the experimental results show that DMF, DMSO and Toluene is good solvent with 94%, 73%, and 44% yields, respectively, under the optimum conditions. Among them, DMF is more preferable. To investigate the effect of temperature on the reaction rate, [3+2] cycloaddition was performed at different temperatures. When the reaction was performed at room temperature, the reaction was found to be inefficient during 12 h (red column). Generally, whilst the reaction temperature was increased to 110 °C, the yield was sustainable.

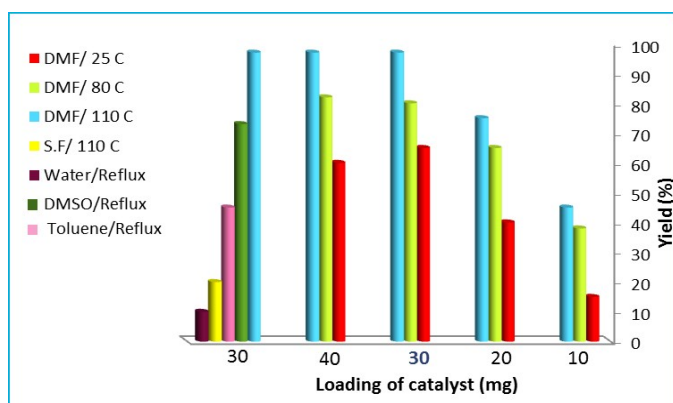


Figure 9. Effects of loading of catalyst, duration of reaction and solvent for the synthesis of 5-Substituted 1H-Tetrazoles (Scheme 4)

And also in order to show the efficiency of this catalytic system further, the synthesis of 5-Substituted 1H-Tetrazoles was investigated in the presence of magnetic Fe₂O₃@DA/Ag hollow sphere. As shown, the optimized reaction conditions (1:1.5 molar ratio of benzonitrile: sodium azide, 30 mg catalyst, in DMF at 110 °C) were used for all organic benzonitrile and the corresponding 5-substituted-1H tetrazoles were prepared within 5-13 h with good to excellent yields.

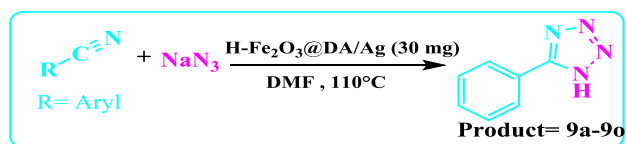


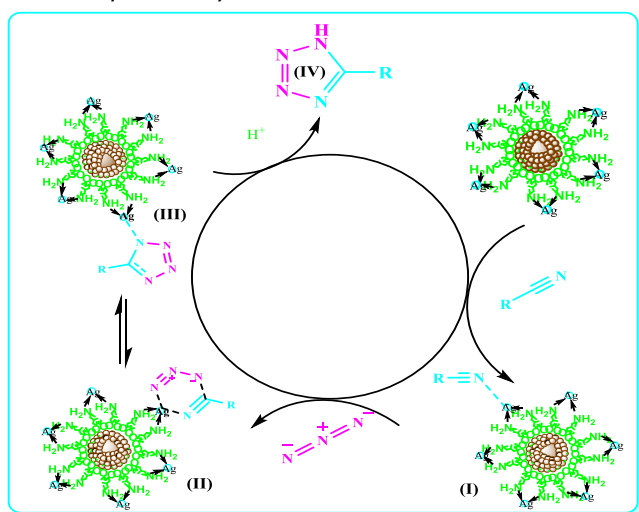
Table 3. Synthesis of 5-substituted-1H-tetrazole from derivatives of aryl cyanide and sodium azide catalyzed by magnetic Fe₂O₃@DA/Ag hollow sphere^a

R	Product	Time (h)	Yield (%) ^b
C ₆ H ₅	9a	7	94
<i>p</i> -O ₂ N-C ₆ H ₄	9b	5	90
<i>p</i> -CH ₃ -C ₆ H ₄	9c	8	89
<i>p</i> -OCH ₃ -C ₆ H ₄	9d	9	86
β-Naphtol	9e	7	85
Α-Naphtol	9f	8	79
<i>m</i> -Cl-C ₆ H ₄	9g	7	85
<i>p</i> -Cl-C ₆ H ₄	9h	8	85
<i>p</i> -Br-C ₆ H ₄	9i	7	87
<i>p</i> -OH-C ₆ H ₄	9j	11	87
<i>p</i> -CN-C ₆ H ₄	9k	5	75
2-Pyridine	9l	6	85
4-Pyridine	9m	5	88
CH ₂ -C ₆ H ₅	9n	13	70
<i>o</i> -NH ₂ - <i>m</i> -NO ₂ -C ₆ H ₄	9o	9	82

^a Reaction condition: nitriles (1.0 mmol), Sodium azide (1.5 mmol), magnetic h-Fe₂O₃@DA/Ag (30 mg), DMF (2 mL), 110 °C

^b Yields are after work-up.

Benzonitrile containing both electron withdrawing and electron donating groups underwent the conversion smoothly. The benzonitrile having electron donating substituents require longer reaction time as donating substituent on aromatic ring decreases the electrophilic character of benzonitrile. Generally, this catalyst has some advantages such as giving the selected three-component reaction a short reaction time, providing excellent yields and offering simple and almost quantitative recovery of the magnetized catalyst in pure form to be re-used in several further runs without appreciable loss in its catalytic activity.



Scheme 5. Plausible mechanism for the synthesis of 5-Substituted 1H-Tetrazoles by h-Fe₂O₃@DA/Ag

By considering results in the literature report, a proposed mechanism for the formation of the 1-substituted tetrazole is shown in scheme 5. It is clear that, silver nanoparticles act as a Lewis acid activating the nitrile groups *via* complexation (I). Therefore, it enhances the electrophilic property of cyanide group, which then reacts with sodium azide to form of intermediate (II). At the end, magnetic h-Fe₂O₃@DA/Ag catalyst-assisted elimination of ethanol from (III) leads to the final product (IV).

Recycling and leaching of the catalyst

As the possibilities of recycling the catalyst are one of the key advantages of organic procedures concerning green chemistry aspects, the catalyst was recycled and reused. In order to study these important features and constancy of the activity of this novel used catalyst system, the catalyzed three-component reaction involving benzaldehyde, piperidine and phenylacetylene was selected as a model reaction and conducted under already secured optimal reaction conditions including the use of the exact amount of optimized quantity of the catalyst. Figure 10 indicates that the heterogeneous catalyst was used for 5 successive times in the new experiments without dramatic yield loss and generates a product with purity similar to that obtained in the first run.

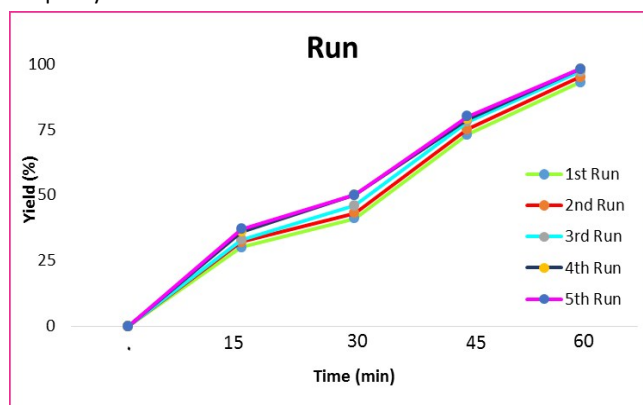


Figure 10. Reusability of the h-Fe₂O₃@DA/Ag catalyst in A³ Coupling

Conclusions

The present work demonstrates a unique and facile approach to the fabrication of Ag-doped nano magnetic-Fe₂O₃@DA Core-Shell Hollow Spheres. The formation mechanism of the core shell nanoparticles was directly related to DA molecules, attached to silver nanoparticles seeds, dissociate from h-Fe₂O₃ surfaces. The phase and structure of the as-obtained were identified by XRD, FT-IR, FE-SEM, EDS, TGA and VSM measurements and shells was clearly revealed by TEM characterizations. Additionally, apparent shell density as physical property was determined using the specific surface area and shell thickness. The nano magnetic γ-Fe₂O₃@DA/Ag hollow sphere product exhibited an excellent catalytic activity for the synthesis of propargylamine by A³, KA² coupling reaction and 1H-tetrazoles via [3+2] cycloaddition. Moreover, this catalyst could be easily separated and reused up to five times with no significant loss of activity and selectivity. The easy reusability of the catalyst without any further purification proved as a high potential candidate for organic reactions. It is

believed that this facile synthesis method reported here can be applied to the preparation of effective catalyst with hollow sphere structure.

Experimental

Materials and instruments

All chemicals, including $\text{FeCl}_3 \cdot 6\text{H}_2\text{O}$, trisodium citrate dihydrate, sodium acetate trihydrate, ethanol, ethylene glycol (EG), PVP, urea, dopamine, AgNO_3 and $\text{NH}_3 \cdot \text{H}_2\text{O}$, were analytical grade reagents, purchased from Sigma-Aldrich, and used without further purification. The progress of the reaction was monitored by TLC on commercial aluminum-backed plates of silica gel 60 F254, visualized, using ultraviolet light. Melting points were determined in open capillaries using an Electrothermal 9100 without further corrections. ^1H NMR and ^{13}C NMR spectra were recorded using a Bruker DRX-400 spectrometer at 400 and 100 MHz respectively. Magnetic- $\text{Fe}_2\text{O}_3@DA/Ag$ hollow sphere was characterized by; FT-IR spectra were obtained with potassium bromide pellets in the range of $400\text{--}4000\text{ cm}^{-1}$ using a Shimadzu 8400s spectrometer; X-ray diffraction (XRD) was detected by Philips using Cu-K α radiation of wavelength 1.54 \AA ; Scanning electron Microscopy, FE-SEM-EDX, analysis was performed using Tescanvega II XMU Digital Scanning Microscope. Samples were coated with gold at 10 mA for 2 min prior to analysis; the magnetic properties were characterized using a vibrating sample magnetometer (VSM, Lakeshore7407) at room temperature. Thermogravimetric analyses (TGA) were analyzed with a LINSEIS model STS PT 16000 thermal analyzer under air atmosphere at a heating rate of $5\text{ }^\circ\text{C min}^{-1}$.

Preparation of Nano magnetic Fe_2O_3 hollow sphere

Hollow magnetic particles were prepared through solvothermal method.⁷⁶ At first, ferric chloride hexahydrate (5 mmol) was dissolved in 70 mL of ethylene glycol (EG) in a flask, followed by the addition of 1.5 mmol of trisodium citrate dehydrate, 30 mmol of sodium acetate (NaAc) and urea (17 mmol). The resulting mixture was stirred vigorously for 1 h, and was transferred to a Teflon-lined stainless-steel autoclave (150 mL capacity), at $220\text{ }^\circ\text{C}$ for 24 h. And after the reaction, the autoclave was cooled to room temperature. The resulting brown product was washed several times with ethanol and deionized water and was finally dried at $80\text{ }^\circ\text{C}$ in the oven for overnight.

Preparation of $h\text{-Fe}_2\text{O}_3@DA$ Core shell

The $h\text{-Fe}_2\text{O}_3@DA$ shells were prepared according to a previously reported method.⁶³ Briefly, (1 g) of the as-prepared Fe_2O_3 hollow spheres were dispersed in 50 mL of deionized water, and later a certain amount of dopamine (1 g) was added to the suspension. Then, the above suspension was

refluxed for 12 h at $100\text{ }^\circ\text{C}$. The final product ($h\text{-Fe}_2\text{O}_3@DA$) was collected from the reaction medium by employing of a magnet, and then washed with acetone and dried at $70\text{ }^\circ\text{C}$.

Loading Ag nanoparticles to obtain $h\text{-Fe}_2\text{O}_3@DA/Ag$

The doping of Ag nanoparticles onto $h\text{-Fe}_2\text{O}_3@DA$ shell was performed as follows.⁶⁴ Initially, 0.06 g of $h\text{-Fe}_2\text{O}_3@DA$ was dispersed in 15 mL of $5 \times 10^{-3}\text{ M}$ $\text{Ag}(\text{NH}_3)_2\text{NO}_3$ solution under stirring at room temperature for 30 minutes. After that, the $[\text{Ag}(\text{NH}_3)_2]^+$ ions were adsorbed onto the surfaces of $h\text{-Fe}_2\text{O}_3@DA$ via the electrostatic attraction. The dispersion was added in 15 mL of ethanol contained PVP (0.1 g), followed by heating the solution by reflux at $70\text{ }^\circ\text{C}$ for 4 h. The final precipitate was collected by magnetic separation, washed three times with a recycle of ethanol and deionized water, and dried at $50\text{ }^\circ\text{C}$ for 12 h.

Investigating of magnetic $\text{Fe}_2\text{O}_3@DA/Ag$ hollow sphere as an efficient nano catalyst in some organic reaction

General procedure for synthesis of 1-(1,3-diphenylprop-2-ynyl)piperidine: (5a)

To a mixture of benzaldehyde (1.0 mmol), piperidine (1.2 mmol) and phenyl acetylene (1.5 mmol) without any solvent, magnetic $h\text{-Fe}_2\text{O}_3@DA/Ag$ (10 mg), was added. The mixture was heated at $90\text{ }^\circ\text{C}$ for 1h (monitored by TLC). And then, the reaction mixture was cooled to room temperature and diluted with hot ethanol (10 ml). Then, the catalyst was separated by an external magnet from the cooled mixture, washed with acetone, dried in the oven and re-used for a consecutive run under the same reaction conditions. The filter was concentrated and the resulting residue was purified by short column chromatography on silica gel to obtain the excellent yield of the desired product.

General procedure for synthesis of 1-phenyl-1H-tetrazole: (9a)

To a mixture of nitrile (1.0 mmol) and NaN_3 (1.5 mmol) in DMF (2 mL), magnetic $h\text{-Fe}_2\text{O}_3@DA/Ag$ (30 mg), was added. The mixture was stirred at $110\text{ }^\circ\text{C}$ for appropriate time until the reaction was completed (monitored by TLC), and then, that was cooled to room temperature and diluted with ethyl acetate (10 ml) and 5 N HCl (20 mL). The catalyst was separated by an external magnet from the cooled mixture, washed with acetone, dried in oven and re-used for a consecutive run under the same reaction conditions. Then, the organic layer was separated, and the aqueous layer was extracted with ethyl acetate (20 mL). The combined ethyl acetate layer was washed with water, dried over anhydrous Na_2SO_4 . The residue was purified by recrystallization or short

column chromatography on silica gel to afford the target products in excellent yield.

General procedure for recycling of magnetic Fe₂O₃@DA/Ag hollow sphere

Recyclability of Fe₂O₃@DA/Ag (10 mg) was examined for the synthesis of propargylamine between benzaldehyde (1.0 mmol), piperidine (1.2 mmol) and phenyl acetylene (1.5 mmol) and under solvent free conditions for 60 minutes at 90 °C. After that, the mixture was washed five times with ethanol, filtered by using external magnet, and dried in air, and then reused for several runs of reactions under identical conditions.

Spectral data of some selected compound

1-(1,3-diphenylprop-2-ynyl)piperidine (table 1, 5a): Pale yellow oily liquid; ¹H NMR (400 MHz, CDCl₃, ppm) δ 1.45-1.49 (m, 2H), 1.58-1.65 (m, 4H), 2.59 (t, 4H), 4.81 (s, 1H), 7.31-7.40 (m, 6H), 7.53-7.55 (m, 2H), 7.65-67 (d, J=7.6 Hz, 2H).

1-(3-phenyl-1-(thiophen-2-yl)prop-2-ynyl)piperidine (table 1, 5g): Yellow solid; mp 50-51 °C (Lit.⁸⁶ 52-53 °C); ¹H NMR (400 MHz, CDCl₃, ppm) δ 1.48-1.52 (m, 2H), 1.63-1.70 (m, 4H), 2.62-2.71 (m, 4H), 5.03 (s, 1H), 7.00 (dd, J¹=J²=3.6 Hz, 1H), 7.25-7.30 (m, 1H), 7.31 (d, J=4.4 Hz, 2H), 7.36-7.38 (m, 3H), 7.54-7.57 (m, 2H); ¹³C NMR (100 MHz, CDCl₃, ppm) δ 24.4, 26.1, 50.6, 58.2, 85.3, 86.9, 123, 125.3, 125.8, 126.2, 128.2, 128.3, 131.8, 144.

1-(3-phenyl-1-(4-(3-phenyl-1-(piperidin-1-yl)prop-2-ynyl)phenyl)prop-2-ynyl)piperidine (table 1, 5h): White solid; mp 157-159 °C (Lit.⁸⁶ 158-160 °C); ¹H NMR (400 MHz, CDCl₃, ppm) δ 1.47 (m, 2H), 1.59-1.63 (m, 4H), 2.59 (m, 4H), 4.81 (s, 1H), 7.33-7.35 (m, 3H), 7.52-7.55 (m, 2H), 7.63 (s, 2H).

1-(1-(naphthalen-3-yl)-3-phenylprop-2-ynyl)piperidine (table 1, 5i): Yellow oil; ¹H NMR (400 MHz, CDCl₃, ppm) δ 1.47-1.51 (m, 2H), 1.60-1.67 (m, 4H), 2.64 (t, 4H), 4.97 (s, 1H), 7.36-7.40 (m, 3H), 7.48-7.52 (m, 2H), 7.58-7.61 (m, 2H), 7.79 (dd, J¹=J²=8.4 Hz, 1H), 7.85-7.91 (m, 3H), 8.11 (s, 1H); ¹³C NMR (100 MHz, CDCl₃, ppm) δ 24.4, 26.2, 50.8, 62.5, 86, 88.1, 123.3, 125.8, 125.9, 126.7, 127.2, 127.5, 127.7, 128.1, 128.12, 131.8, 132.9, 133.1, 136.3.

N,N-diethyl-1,3-diphenylprop-2-yn-1-amine (table 1, 5r): Pale yellow oily liquid; ¹H NMR (400 MHz, CDCl₃, ppm) δ 1.04 (m, 6H), 2.36-2.62 (m, 4H), 5.19 (s, 1H), 7.15-7.27 (m, 4H), 7.29-7.38 (m, 3H), 7.39-7.41 (m, 2H).

4-(3-phenylprop-2-ynyl)morpholine (table 1, 6c): yellow oil; ¹H NMR (400 MHz, CDCl₃, ppm) δ 2.64-2.67 (m, 6H), 3.52 (s, 3H), 3.69-3.71 (m, 1H), 3.77-3.79 (m, 6H), 7.28-7.31 (m, 4H), 7.43-7.46 (m, 2H).

1-(1-cyclohexyl-3-phenylprop-2-ynyl)pyrrolidine (table 1, 6i): Colorless liquid; ¹H NMR (400 MHz, CDCl₃, ppm) δ 1.05-1.36 (m, 5H), 1.56-1.63 (m, 2H), 1.75-1.79 (m, 6H), 1.82-2.10 (m, 4H), 2.5-2.98 (m, 4H), 3.36-3.38 (d, J = 7.6 Hz, 1H), 7.14-7.33 (m, 3H), 7.50-7.63 (m, 2H). ¹³C NMR (100 MHz, CDCl₃, ppm) δ 24.9, 26.9, 27.1, 28.3, 32.7, 33, 42.9, 51.1, 61.1, 86.1, 88.9, 125.9, 128.9, 129.8, 132.6.

4-(1-phenylhex-1-yn-3-yl)morpholine (Table 1, 6m): Yellow oil; ¹H NMR (400 MHz, DMSO-*d*₆, ppm) δ 0.97 (m, 3H), 1.45-1.75 (m,

4H), 2.67-2.70 (m, 2H), 2.79-2.83 (m, 2H), 3.82-4.13 (m, 1H), 4.15-4.17 (m, 4H), 7.46-7.50 (m, 3H), 7.62-7.64 (m, 2H). ¹³C NMR (100 MHz, DMSO-*d*₆, ppm) δ 10.39/C6RA18810A

1-(1-(2-p-tolylethynyl)cyclohexyl)piperidine (Table 2, 8e): Yellow oil; ¹H NMR (400 MHz, CDCl₃, ppm) δ 1.39-1.93 (m, 16H), 2.17-2.20 (m, 2H), 2.53 (s, 3H), 2.73-2.83 (m, 2H), 7.26-7.27 (m, 3H), 7.46-7.48 (m, 2H); ¹³C NMR (100 MHz, CDCl₃, ppm) δ 21.32, 23.4, 24.4, 25, 26.7, 37.6, 47.9, 58.8, 85.4, 92.1, 123, 127.6, 128.3, 133.

4-(1-(2-phenylethynyl)cyclohexyl)morpholine (Table 2, 8f): Pale yellow oily liquid; ¹H NMR (400 MHz, CDCl₃, ppm) δ 1.28-1.30 (m, 1H), 1.52 (m, 2H), 1.63-1.67 (m, 3H), 1.73 (br.s, 2H), 2.03-2.05 (m, 2H), 2.74 (br.s, 4H), 3.78 (br.s, 4H), 7.27 (m, 3H), 7.44-7.45 (m, 2H), ¹³C NMR (100 MHz, CDCl₃, ppm) δ 22.7, 25.7, 35.4, 46.6, 58.8, 67.4, 86.4, 89.8, 123.4, 127.7, 128.1, 131.7.

4-(1-(4-fluorophenyl)ethynyl)cyclohexyl)morpholine (Table 2, 8i): Yellow oil; ¹H NMR (400 MHz, DMSO-*d*₆, ppm) δ 1.26-1.34 (m, 1H), 1.57-1.62 (m, 2H), 1.69-1.78 (m, 3H), 1.80-1.86 (m, 2H), 2.00-2.02 (m, 2H), 2.78 (s, 4H), 3.70 (br.t, J = 4.2 Hz, 4H), 6.97-7.00 (t, J = 8.6 Hz, 2H), 7.32-7.40 (m, 2H);

5-Phenyl-1H-tetrazole (Table 3, 9a): White solid; mp 213-215 °C (Lit.⁸⁸ 214-215 °C); ¹H NMR (400 MHz, DMSO-*d*₆, ppm) δ 7.68 (s, 3H, Ph), 7.92 (s, 2H, Ph); ¹³C NMR (100 MHz, DMSO-*d*₆, ppm) δ 126.6, 128.6, 130.3, 134.6, 155.

5-(4-Nitrophenyl)-1H-tetrazole (Table 3, 9b): Yellow solid; mp 218-219 °C (Lit.⁸⁸ 220-222 °C); ¹H NMR (400 MHz, DMSO-*d*₆, ppm) δ 8.30 (d, 2H, J 8.4, Ph), 8.39 (d, 2H, J 8.8, Ar-H); ¹³C NMR (100 MHz, DMSO-*d*₆, ppm) δ 127.6, 129.1, 131, 149.5.

5-(4-Methylphenyl)-1H-tetrazole (Table 3, 9c): White solid; mp 249-251 °C (Lit.⁸⁸ 247-249 °C); ¹H NMR (250 MHz, DMSO-*d*₆, ppm) δ 2.35 (s, 3H, CH₃), 7.37 (d, 2H, J 7.6 Hz, Ph), 7.90 (d, 2H, J 7.5 Hz, Ph).

5-(3-Chlorophenyl)-1H-tetrazole (Table 3, 9g): White solid; mp 138-140 °C (Lit.⁸³ 137-139 °C); ¹H NMR (250 MHz, DMSO-*d*₆, ppm) δ 7.55 (m, 2H, Ph), 7.96 (d, 1H, J 7.6, Ph), 7.99 (s, 1H); ¹³C NMR (62.9 MHz, DMSO-*d*₆, ppm) δ 125.4, 126.2, 126.4, 130.7, 131.1, 133.9, 154.6.

5-(4-Chlorophenyl)-1H-tetrazole (Table 3, 9h): White solid; mp 251-253 °C (Lit.⁸⁸ 251-252 °C); ¹H NMR (400 MHz, DMSO-*d*₆, ppm) δ 7.61 (d, 2H, J 8.4, Ph), 8.09 (d, 2H, J 8.8, Ph).

5-(4-Hydroxyphenyl)-1H-tetrazole (Table 3, 9j): White solid; mp 235 °C (Lit.⁸⁸ 233-234 °C); ¹H NMR (400 MHz, DMSO-*d*₆, ppm) δ 6.91 (d, 2H, J 8.4, Ph), 7.58 (d, 2H, J 8.4, Ph), 10.11 (s broad, OH); ¹³C NMR (100 MHz, DMSO-*d*₆, ppm) δ 116.1, 117.4, 128.8, 153.2, 159.8.

4-(1H-tetrazol-5-yl)-benzotrile (Table 3, 9k): White solid; mp 257-259 °C (Lit.⁸⁹ 258-260 °C); ¹H NMR (250 MHz, DMSO-*d*₆, ppm) δ 8.06 (d, 2H, J 7.1, Ph), 8.19 (d, 2H, J 8.6, Ar-H); ¹³C NMR (62.9 MHz, DMSO-*d*₆, ppm) δ 113.3, 118.1, 127.6, 128.7, 133.1, 155.2, 162.2.

2-(1H-tetrazol-5-yl)pyridine (Table 3, 9l): White solid; mp 210-213 °C (Lit.⁹⁰ 211-212 °C); ¹H NMR (400 MHz, DMSO-*d*₆, ppm) δ 7.75 (s, 1H, Ph), 8.07 (s, 1H, Ph), 8.20 (d, 1H, J 8.4 Ph), 8.63 (s, 1H).

4-(1H-tetrazol-5-yl)pyridine (Table 3, 9m): White solid; mp 256-258 °C (Lit.⁹¹ 256-258 °C); ¹H NMR (250 MHz, DMSO-*d*₆, ppm) δ 8.10 (d, 2H, J 6.0, Ph), 8.77 (d, 2H, J 6.5, Ph); ¹³C NMR (62.9 MHz, DMSO-*d*₆, ppm) δ 120.9, 121.3, 133.8, 149.9, 165.7.

Acknowledgements

The authors wish to gratefully acknowledge the partial support of this study by Semnan University and Amirkabir University of Technology (AUT) Research Council.

Notes and references

- H. Deng, X. L. Li, Q. Peng, X. Wang, J. P. Chen and Y. D. Li, *Angew. Chem., Int. Ed.* 2005, **44**, 2782.
- A. H. Lu, E. L. Salabas and F. Schuth, *Angew. Chem., Int. Ed.* 2007, **46**, 1222.
- H. Luo, K. Huang, B. Sun and J. X. Zhong, *Electrochim. Acta.*, 2014, **149**, 11.
- B. D. Wang, J. Hai, Q. Wang, T. R. Li and Z. Y. Yang, *Angew. Chem. Int. Ed.*, 2011, **50**, 3063.
- Y. Fu, R. M. Wang, J. Xu, J. Chen, Y. Yan, A. V. Narlikar and H. Zhang, *Chem. Phys. Lett.*, 2003, **379**, 373.
- Y. Y. Fu, J. Chen and H. Zhang, *Chem. Phys. Lett.*, 2001, **350**, 491.
- J. J. Wu, Y. L. Lee, H. H. Chiang and D. K. P. Wong, *J. Phys. Chem. B. Lett.*, 2006, **110**, 18108.
- V. Salgueiriño-Maceira, M. Spasova and M. Farle, *Adv. Funct. Mater.*, 2005, **15**, 1036.
- C. R. Gong, D. R. Chen, X. L. Jiao and Q. L. Wang, *J. Mater. Chem.*, 2004, **14**, 905.
- L. P. Zhu, H. M. Xiao and S. Y. Fu, *Cryst. Growth Des.*, 2007, **7**, 177.
- L. Liu, H. Z. Kou, W. L. Mo, H. J. Liu and Y. Q. Wang, *J. Phys. Chem. B*, 2006, **110**, 15218.
- X. L. Hu, J. C. Yu and J. M. Gong, *J. Phys. Chem. C*, 2007, **111**, 11180.
- X. G. Wen, S. H. Wang, Y. Ding, Z. L. Wang and S. H. Yang, *J. Phys. Chem. B*, 2005, **109**, 215.
- B. Hou, Y. S. Wu, L. L. Wu, Y. C. Shi, K. Zou and H. D. Gai, *Mater. Lett.*, 2006, **60**, 3188.
- Y. Shi, M. M. Shi, Y. Q. Qiao, J. P. Tu and H. Z. Chen, *Nanotechnol.*, 2012, **23**, 395601.
- B. Y. Geng, F. M. Zhan, H. Jiang, Y. J. Guo and Z. J. Xing, *Chem. Commun.*, 2008, 5773.
- J. Y. Zhong, C. B. Cao, Y. Y. Liu, Y. N. Li and W. S. Khan, *Chem. Commun.*, 2010, **46**, 3869.
- Y. Wang, Q. S. Zhu and L. Tao, *Cryst. Eng. Comm.*, 2011, **13**, 4652.
- M. Hu, S. Furukawa, R. Ohtani, H. Sukegawa, Y. Nemoto, J. Reboul, S. Kitagawa and Y. Yamauchi, *Angew. Chem., Int. Ed.*, 2012, **51**, 984.
- M. B. Gawande, Y. Monga, R. Zboril and R. K. Sharma, *Coord. Chem. Rev.*, 2015, **288**, 118.
- W. Ostwald, *Z. Phys. Chem.*, 1897, **22**, 289.
- W. Cheng, K. B. Tang, Y. X. Qi, J. Sheng and Z. P. Liu, *J. Mater. Chem.*, 2010, **20**, 1799.
- A. D. Smigelskas and E. O. Kirkendall, *Trans. AIME*, 1947, **171**, 130.
- G. H. Jaffari, A. Ceylan, H. P. Bui, T. P. Beebe Jr., S. Ozcan and S. I. Shah, *J. Phys.: Condens. Matter.*, 2012, **24**, 336004.
- B. Jia and L. Gao, *J. Phys. Chem. C*, 2008, **112**, 666.
- P. Hu, L. Yu, A. Zuo, C. Guo and F. Yuan, *J. Phys. Chem. C*, 2009, **113**, 900.
- S. W. Kim, M. Kim, W. Y. Lee and T. Hyeon, *J. Am. Chem. Soc.*, 2002, **124**, 7642.
- B. Tan and S. E. Rankin, *Langmuir*, 2005, **21**, 8180-8187.
- Y. Ding, Y. Hu, X. Jiang, L. Zhang and C. Yang, *Angew. Chem., Int. Ed.*, 2004, **43**, 6369.
- J. Chattopadhyay, T. S. Pathak, R. Srivastava and A. C. Singh, *Electrochimica Acta.*, 2015, **167**, 429.
- H. Lv, G. Ji, W. Liu, H. Zhang and Y. Du, *J. Mater. Chem. C*, 2015, **3**, 10232.
- Y. Yang, W. Zhang, Y. Zhang, A. Zheng, H. Sun, Xi. Li, S. Liu, P. Zhang and X. Zhang, *Nano Research*, 2015, **10**, 1007/s12274-015-0840-9.
- C. Zhou, K. Huang, L. Yuan, W. Feng, X. Chu, Zh. Geng, X. Wu, L. Wang and Sh. Feng, *New J. Chem.*, 2015, **39**, 2413.
- W. Yan, Zh. Yang, W. Bian and R. Yang, *Carbon*, 2015, **92**, 74.
- Y. Gu, X. Liu, T. Niu and J. Huang, *Mater. Res. Bull.*, 2010, **45**, 536.
- M. K. Kim, D. W. Kim, D. W. Shin, S. J. Seo, H. K. Chung and J. B. Yoo, *Phys. Chem. Chem. Phys.*, 2015, **17**, 2416.
- M. Ohnishi, Y. Kozuka, Q. L. Ye, H. Yoshikawa, K. Awaga, R. Matsuno, M. Kobayashi, A. Takahara, T. Yokoyama, Sh. Bandow and S. Iijima, *J. Mater. Chem.*, 2006, **16**, 3215.
- T. Yao, H. Wang, Q. Zuo, J. Wu, B. Xin, F. Cui and T. Cui, *J. Colloid. Interface Sci.*, 2015.
- P. Wang, H. Zhu, M. Liu, J. Niu, B. Yuan, R. Li and J. Ma, *RSC Adv.*, 2014, **4**, 28922.
- P. Damier, E. C. Hirsch, Y. Agid and A. M. Graybiel, *Brain*, 1999, **122**, 1437.
- O. L. Lopez, G. Smith, C. C. Meltzer and J. T. Becker, *Neuropsy. Neuropsy. Behav. Neurol.*, 1999, **12**, 184.
- V. Polshettiwar, B. Baruwati and R. S. Varma, *Green Chem.*, 2009, **11**, 127.
- B. Reddy Vaddula, A. Saha, J. Leazer and R. S. Varma, *Green Chem.*, 2012, **14**, 2133.
- A. Saha, J. Leazer and R. S. Varma, *Green Chem.*, 2012, **14**, 67.
- D. Losic, Y. Yu, M. Sinn Aw, S. Simovic, B. Thierry and J. Addai-Mensah, *Chem. Commun.*, 2010, **46**, 6323.
- R. B. Nasir Baig and R. S. Varma, *Chem. Commun.*, 2012, **48**, 2582.
- M. Harmata, *Silver in Organic Chemistry*, John Wiley & Sons, Hoboken, 2010.
- V. A. Peshkov, O. P. Pereshivko and E. V. Van der Eycken, *Chem. Soc. Rev.*, 2012, **41**, 3790.
- T. Harada, T. Fujiwara, K. Iwazaki and L. A. Oku, *Org. Lett.*, 2000, **2**, 1855.
- C. H. Ding, D. D. Chen, Z. B. Luo, L. X. Dai and X. L. Hou, *Synlett*, 2006, 1272.
- C. M. Wei, J. T. Mague and C. J. Li, *Proc. Natl. Acad. Sci.*, 2004, **101**, 5749.
- T. Zeng, L. Yang, R. Hudson, G. Song, A. R. Moores and C. J. Li, *Org. Lett.*, 2011, **13**, 442.
- H. Sharghi, R. Khalifeh, F. Moeini, M. H. Beyzavi, A. Salimi Beni and M. M. Doroodmand, *J. Iran. Chem. Soc.*, 2011, **8**, 89.
- F. Nemat, A. Elhampour, H. Farrokhi and M. B. Natanzi, *Catal Commun.*, 2015, **66**, 15.
- S. Sakaguchi, T. Kubo and Y. Ishii, *Angew. Chem. Int. Ed.*, 2001, **113**, 2602.
- K. Namitharan and K. Pitchumani, *Eur. J. Org. Chem.*, 2010, **2010**, 411.
- T. Zeng, W. Chen, C. M. Cirtiu, A. Moores, G. Song and C. J. Li, *Green Chem.*, 2010, **12**, 570.
- T. Hashimoto and K. Maruoka, *Chem. Rev.*, 2015, **115**, 5366.
- J. M. Longmire, B. Wang, and X. Zhang, *J. Am. Chem. Soc.*, 2002, **124**, 13400.
- A. Sejr Gothelf, K. V. Gothelf, R. G. Hazell and K. Anker Jørgensen, *Angew. Chem., Int. Ed.*, 2002, **41**, 4236.
- X. H. Chen, W. Q. Zhang and L. Z. Gong, *J. Am. Chem. Soc.*, 2008, **130**, 5652.
- F. Shi, R. Y. Zhu, X. Liang and S. J. Tu, *Adv. Synth. Catal.*, 2013, **355**, 2447.
- D. Kong, Y. Liu, J. Zhang, H. Li, X. Wang, G. Liu, B. Li and Z. Xud, *New J. Chem.*, 2014, **38**, 3078.
- A. Coca and E. Turek, *Tetrahedron Lett.*, 2014, **4**, 49.
- Z. Wang, Z. Liu and S. H. Cheon, *Bull. Korean Chem. Soc.*, 2015, **36**, 198.

- 66 F. Nemati, A. Elhampour and S. Zulfaghari, *Phosphorus Sulfur Silicon Relat. Elem.*, 2015, **190**, 1692.
- 67 F. Nemati, M. M. Heravi and R. Saeedirad, *Chin. J. Catal.*, 2012, **33**, 1825.
- 68 F. Nemati, M. Golmohammadi Afkham and A. Elhampour, *Green Chem. Lett. Rev.*, 2014, **7**, 79.
- 69 F. Nemati and R. Saeedirad, *Chin. Chem. Lett.*, 2013, **24**, 370.
- 70 F. Nemati and S. Sabaqian, *J. Saudi. Chem. Soc.*, 2014, doi:10.1016/j.jscs.2014.04.009.
- 71 F. Nemati, S. H. Nikkhah and A. Elhampour, *Chin. Chem. Lett.*, 2015, **26**, 1397.
- 72 F. Nemati, M. M. Heravi and A. Elhampour, *RSC Adv.*, 2015, **5**, 45775.
- 73 A. Amoozadeh, M. Malmir, N. Koukabi and S. Otokesh, *J. Chem. Res.*, 2015, **39**, 694.
- 74 E. Tabrizian, A. Amoozadeh, S. Rahmani, E. Imanifar, S. Azhari and M. Malmir, *Chin. Chem. Lett.*, 2015, **26**, 1278.
- 75 S. Otokesh, N. Koukabi, E. Kolvari, A. Amoozadeh, M. Malmir and S. Azhari, *S. Afr. J. Chem.*, 2015, **68**, 15.
- 76 S. Zhang, F. Ren, W. Wu, J. Zhou, X. Xiao, L. Sun, Y. Li and C. Jiang, *Phys. Chem. Chem. Phys.*, 2013, **15**, 8228.
- 77 J. Safari and Z. Zarnegar, *J. Mol. Catal. A: Chem.*, 2013, **379**, 269.
- 78 C. Takai, H. Watanabe, T. Asai and M. Fujii, *Colloids Surf., A*, 2012, **404**, 101.
- 79 C. Wei, Z. Li and C. J. Li, *Org. Lett.*, 2003, **5**, 4473.
- 80 X. Zhou, Y. Lu, L. L. Zhai, Y. Zhao, Q. Liu and W. Y. Sun, *RSC Adv.*, 2013, **3**, 1732.
- 81 W. Yan, R. Wang, Z. Xu, J. Xu, L. Lin, Z. Shen and Y. Zhou, *J. Mol. Catal. A: Chem.*, 2006, **255**, 81.
- 82 N. Salam, A. Sinha, A. Singha Roy, P. Mondal, N. R. Jana and S. M. Islam, *RSC Adv.*, 2014, **4**, 10001.
- 83 O. Prakash, H. Joshi, U. Kumar, A. K. Sharma and A. K. Singh, *Dalton Trans.*, 2015, **44**, 1962.
- 84 M. A. Aleem Ali, A. El-Remaily and H. A. Hamad, *J. Mol. Catal. A: Chem.*, 2015, **404**, 148.
- 85 P. Mani, A. C. Sharma, S. Kumar and S. K. Awasthi, *J. Mol. Catal. A: Chem.*, 2014, **392**, 150.
- 86 M. Tajbakhsh, M. Farhang, M. Baghbanian, R. Hosseinzadeh and M. Tajbakhsh, *New J. Chem.*, 2015, **39**, 18275. View Article Online
DOI: 10.1039/C5NJ01827G
- 87 A. Khalafi-Nezhad and S. Mohammadi, *RSC Adv.*, 2013, **3**, 4362. C6RA18810A
- 88 G. A. Meshrama, S. S. Deshpandea, P. A. Wagha and V. A. Vala, *Tetrahedron Lett.*, 2014, **55**, 3557.
- 89 A. I. Azath, P. Suresh and K. Pitchumani, *New J. Chem.*, 2012, **36**, 2334.
- 90 V. Rama, K. Kanagaraj and K. Pitchumani *J. Org. Chem.*, 2011, **76**, 9090.
- 91 M. Esmailpour, J. Javidi, F. Nowroozi Dodeji and M. Mokhtari Abarghoui, *J. Mol. Catal. A: chem.*, 2014, **393**, 18.

Graphical abstract

View Article Online
DOI: 10.1039/C6RA18810A